CHEMISTRY OF
MATERIALS
Communication

Chem. Mater. **2009,** *21,* 5569–5571 5569
DOI:10.1021/cm902293p

Template-Free Growth of Micro/Nanocrystals of Magnetic Molecular Conductor by Electrocrystallization on Platinum Electrode

Xiangfeng Shao,*[,†] Yuhta Yamaji,[†] Toyonari Sugimoto,*[,†]
Hisashi Tanaka,[‡] Dominique de Caro,[§,⊥] and
Lydie Valade[§,⊥]

[†] *Department of Chemistry, Graduate School of Science, Osaka Prefecture University, Osaka 599-8570, Japan.,* [‡] *Nanotechnology Research Institute, AIST, Central2 Umezono, Tsukuba, Ibaraki 305-8568, Japan,* [§] *CNRS, LCC (Laboratoire de Chimie de Coordination), 205, route de Narbonne, F-31077 Toulouse, France, and* [⊥] *Université de Toulouse, UPS, INPT, LCC, F-31077 Toulouse, France*

Received July 27, 2009
Revised Manuscript Received October 26, 2009

Molecular conductors exhibit a variety of interesting properties, including superconductivity,[1] magnetism,[2] and multiple instabilities under external stimuli such as light,[3] temperature,[4] and so on. Molecular conductors are usually prepared and studied as single crystals, which are principally obtained by electrochemical oxidation of donor molecules in the presence of corresponding supporting electrolytes. Because the single-crystalline samples are difficult to be integrated to devices, the micro/nanometer scale molecular conductors are required. Nanowires and/or nanosticks of the molecular conductors are still rare,[5] and they have been prepared by electrocrystallization using the electrodes with templates such as porous aluminum oxide[6] and phospholipid multilamella.[7]To obtain pure nanowires, we have to remove the template, which is difficult in most cases because the ordered structures are often altered or even destroyed during the template removal. Recently, the growth of nanosticks of molecular conductors has been developed by virtue of supramolecular assembly, where the one-dimesional (1D) stacks of conducting component are formed within the space of the insulating networks.[8] In this case, the insulating networks may also play a role as a kind of template.

On the other hand, it is possible to prepare the 1D micro/nanocrystalline molecular conductors without any templates by careful design of donor molecules. Such a donor molecule should have the strong tendency to assemble along a specific direction. We have noticed that the bent donor molecules (see Figure 1a) with relatively large arcs, EDO-EDSe-TTFVS (**1**),[4c,9] EDO-EDSe-TTFVO (**2**),[4c] and EDT-EDSe-TTFVS (**3**),[10] almost absolutely form the highly 1D columns in the partially oxidized state. However, the electrochemical oxidation of these donor molecules afforded only long platelet single crystals so far. Here we report the facile and reproducible formation of micro/nanometer crystalline 2:1 radical cation salt of a bent donor molecule EDT-EDSe-DSDTFVS (**4**) with $\mathrm{FeCl_4}^-$ ion on the native platinum rod. The electronic transport and magnetic properties of the micro/nanocrystals of $\mathbf{4}_2\cdot\mathrm{FeCl_4}$ will also be reported. To the best of our knowledge, this is the first case to prepare the micro/nanocrystalline molecular conductors by electrocrystallization using a conventional Pt electrode without any template.

A solution of **4** (2.0 mg) and $\mathrm{Bu_4N\cdot FeCl_4}$ (35 mg) in the mixed solvent of chlorobenzene−ethanol (10 mL, 9: 1, *v*/*v*) was introduced into an H-type electrochemical cell. Both the cathode and anode were Pt rods with the diameter of 1 mm. Electrocrystallization was performed by applying a constant current of 1.0 μA at 30 °C under an argon

---

*Corresponding author. E-mail: shao_xf@hotmail.com (X.S.); toyonari@c.s.osakafu-u.ac.jp (T.S.).

(1) Ishiguro, T; Yamaji, K; Saito, G. *Organic Superconductors*; Springer: New York, 1998.

(2) (a) Coronado, E.; Day, P. *Chem. Rev.* **2004**, *104*, 5419–5448. (b) Enoki, T.; Miyazaki, A. *Chem. Rev.* **2004**, *104*, 5449–5478. (c) Kobayashi, H.; Cui, H.-B.; Kobayashi, A. Chem. Rev. **2004**, *104*, 5265−5288, and references therein.

(3) Collet, M.; Guerin, L.; Uchida, N.; Fukuya, S.; Shimoda, H.; Ishikawa, T.; Matsuda, K.; Hasegawa, T.; Ota, A.; Yamochi, H.; Saito, G.; Tazaki, R.; Adachi, S.; Koshihara, S. *Science* **2005**, *307*, 86–89.

(4) (a) Ota, A.; Yamochi, H.; Saito, G. *J. Mater. Chem.* **2002**, *12*, 2600–2602. (b) Shao, X.; Nakano, Y.; Sakata, M.; Yamochi, H.; Yoshida, Y.; Maesato, M.; Uruichi, M.; Yakuchi, K.; Otsuka, A.; Saito, G.; Koshihara, S.; Tanaka, K. *Chem. Mater.* **2008**, *20*, 7551–7562. (c) Shao, X.; Yamaji, Y.; Fujiwara, H.; Sugimoto, T. *J. Mater. Chem.* **2009**, *19*, 5837–5844.

(5) (a) de Caro, D.; Malfant, I.; Savy, J.-P.; Valade, Y. *J. Phys.: Condens. Matter* **2008**, *20*, 184012/1–10. (b) Xing, L.; Li, D.; Hu, S.; Jing, H.; Fu, H.; Mai, Z.; Li, M. *J. Am. Chem. Soc.* **2006**, *128*, 1749–1754.

(6) (a) Cui, G.; Xu, W.; Guo, C.; Xiao, X.; Xu, H.; Zhang, D.; Jiang, L.; Zhu, D. *J. Phys. Chem. B* **2004**, *108*, 13638–13642. (b) Ji, H.-X.; Hu, J.-S.; Tang, Q.-X.; Hu, W.-P.; Song, W.-G.; Wan, L.-J. *Adv. Mater.* **2006**, *18*, 2753–2757.

(7) Savy, J.-P.; de Caro, D.; Faulman, C.; Valade, L.; Almeida, M.; Koike, T.; Fujiwara, H.; Sugimoto, T.; Fraxedas, J.; Ondarçuchu, T.; Pasquier, C. *New J. Chem.* **2007**, *31*, 519–527.

(8) (a) Yamamoto, H. M.; Yamamura, J.; Kato, R. *J. Am. Chem. Soc.* **1998**, *120*, 5905–5913. (b) Yamamoto, H. M.; Maeda, R.; Yamamura, J.; Kato, R. *J. Mater. Chem.* **2001**, *11*, 1034–1041. (c) Yamamoto, H. M.; Kosaka, Y.; Maeda, R.; Yamamura, J.; Nakao, A.; Nakamura, T.; Kato, R. *ACS Nano* **2008**, *2*, 143–155.

(9) The black platelet single crystals of 2:1 radical cation salts of EDO-EDSe-TTFVS (**1**) with $\mathrm{AsF_6}^-$, $\mathrm{PF_6}^-$, and $\mathrm{ClO_4}^-$ ions were obtained by electrocrystallization of **1** in the presence of an appropriate supporting electrolyte at 45 °C in chlorobenzene−ethanol (10 mL, 9: 1, *v*/*v*). In the crystal of these salts, the donor molecules formed 1D columns along the molecular face-to-face direction. All of these salts show semiconducting behavior with the room temperature conductivities of ca. 2 S cm^{-1}.

(10) The black platelet single crystals of 2:1 radical cation salts of EDT-EDSe-TTFVS (**3**) with $\mathrm{FeCl_4}^-$ and $\mathrm{FeBr_4}^-$ ions as well as the 3:1 salts of **3** with $\mathrm{ClO_4}^-$ ion were obtained by electrochemical oxidation of **3** in the presence of appropriate supporting electrolyte at 45 °C in chlorobenzene−ethanol (10 mL, 9: 1, *v*/*v*). Similar to the crystal structures of the salts based on **1**, the donor molecules in these salts also formed 1D columns along the molecular face-to-face direction. All of these salts show semiconducting behavior with the room temperature conductivities of ca. 5 S cm^{-1}. The d-spins of $\mathrm{FeX_4}^-$ ions in the $\mathbf{3}_2\cdot\mathrm{FeX_4}$ (X = Cl, Br) show relatively strong antiferromagnetic interactions.

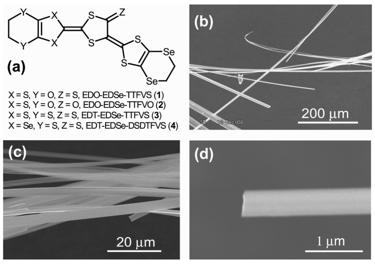

Figure 1. (a) Chemical structures of bent donor molecules; (b−d) SEM images of micro/nanocrystals of $\mathbf{4}_2\cdot\mathrm{FeCl}_4$ corresponding to the length, width, and thickness of micro/nanocrystals, respectively.

atmosphere. Within a week, very thin and long black fibrils were formed on the surface of the anodic Pt rod. At the temperatures lower than 20 °C, a large amount of fibrils covered the surface of anodic Pt rod. The length of fibrils was reduced, whereas the thickness and width of fibrils remained nearly the same. On the basis of the SEM-EDX, the fibrils were proved to be a radical cation salt and the composition of which was determined to be $\mathbf{4}_2\cdot\mathrm{FeCl}_4$. The SEM-EDX result was S:Cl:Fe:Se = 14.37:5.03:1:8.30 ≈ 14:4:1:8 (see Figure S1 in the Supporting Information). Note that the electrochemical oxidation of **4** at 45 °C applying a constant current of 0.2 μA afforded black platelet bulk crystals of $\mathbf{4}_2\cdot\mathrm{FeCl}_4$ with typical size of $0.5 \times 0.2 \times 0.02$ mm^3. X-ray single-crystal diffraction was carried out for both micro and bulk crystals, while their crystal structures could not be solved due to the poor quality of crystals. The unit cell parameters for both micro and bulk crystals are similar within the standard deviations: a = 7.187(7) Å, b = 17.17(1) Å c = 43.91(4) Å, α = 78.08(8)°, β = 82.05(6)°, γ = 79.24(7)°, V = 4578.2(8) Å^3. The a-, b-, and c-axes are colinear to the width, length, and thickness directions of single crystal, respectively. The powder X-ray diffraction (XRD) patterns for the bulk and micro/nano crystals are almost identical (see Figure S3 in the Supporting Information). Since the bent donor molecules with large arcs always form the 1D columns without polymorphisms in the partially oxidized state. The same unit cell parameters and powder XRD patterns for the micro/nano and bulk crystals of $\mathbf{4}_2\cdot\mathrm{FeCl}_4$ indicate that the crystal structures of these two species should be same in principle.

As demonstrated by the large-area SEM imaging shown in Figure 1b, ultralong micro/nanocrystals of $\mathbf{4}_2\cdot\mathrm{FeCl}_4$ were obtained. The maximum length of crystals is more than 3 cm with good flexibility, that can be wrapped to a circle without breaking the crystals. The width (Figure 1c) and thickness (Figure 1d) of crystals are in the micrometer and nanometer scales, respectively.

Figure 2a depicts the AFM images of micro/nanocrystals of $\mathbf{4}_2\cdot\mathrm{FeCl}_4$. The surface of micro/nanocrystals shows stepwise morphology. The height of each step is around 4−6 nm, suggesting that the micro/nanocrystals are intrinsically composed of nano flakes with the thickness of ca. 5 nm. The flakes adhered to each other along the crystal c-axis, which may cause the disorder along this direction. As a result, we could not solve the crystal structure of the salt. Moreover, the thickness of nano flake is very close to the length of the crystal c-axis (4.4 nm). By careful comparison of the unit cell parameters of $\mathbf{4}_2\cdot\mathrm{FeCl}_4$ with those of the radical cation salts based on **1**,[4c,9] **2**,[4c] and **3**,[10] the c-axis of $\mathbf{4}_2\cdot\mathrm{FeCl}_4$ should correspond to the donor-anion direction. The a- and b-axes are along the side-by-side and face-to-face arrays of donor molecules, respectively.

On the basis of the above results, a schematic display for the formation of micro/nanocrystals of $\mathbf{4}_2\cdot\mathrm{FeCl}_4$ is shown in Figure 2b. As is well-known, the crystal growth is a competitive process between the thermodynamic and kinetic factors. In the early stage of $\mathbf{4}_2\cdot\mathrm{FeCl}_4$ nucleation, a unit cell of radical cation salt is formed. Under the relatively high temperature (45 °C) and low current (0.2 μA), the thermodynamic factors play the dominant role. The donor molecules **4** and counter FeCl_4^- ions diffuse from the bulk solution and adsorb onto each direction of the unit cell. Accordingly, the bulk crystals are formed. On the other hand, when a lower temperature (30 °C) and a higher current (1.0 μA) are applied to the electrochemical oxidation, the diffusion rates of donor molecules and counteranions are suppressed. In this case, the kinetic factors control the crystal growth. Driven by the large current density along the face-to-face array, the donor molecules **4** are quickly electrochemically oxidized and adsorb to this prior direction.[5a,11] The counter FeCl_4^- ions migrate to combine with $(\text{EDT-EDSe-DSDTFVS})_2^{\bullet+}$ species, giving rise to the formation of ultralong micro/nanocrystals of $\mathbf{4}_2\cdot\mathrm{FeCl}_4$. Because the donor−anion interactions are relatively weak in the alternatingly layered structures of radical cation salts, the rate of crystal growth along this direction is the lowest among the three directions of the crystal. Consequently, only one unit cell was generated along this direction during the crystal growth, as demonstrated by the AFM images. At temperatures below 20 °C, the solubility of the $\mathbf{4}_2\cdot\mathrm{FeCl}_4$ radical cation salt was further decreased. The nucleation became more rapid to cover the surface of the anodic Pt rod, that resulted in the suppression of the further elongation of the fibrils. The best condition to obtain the ultralong micro/nanocrystals of $\mathbf{4}_2\cdot\mathrm{FeCl}_4$ is electrochemical oxidation of **4** at 30 ± 3 °C by applying a constant current of 1.0 ± 0.2 μA.Note that no needle-like crystals of $\mathbf{4}_2\cdot\mathrm{FeCl}_4$ could be obtained under any conditions. Although micro/nanocrystals of molecular conductors have been successfully prepared by using the templates,[5−8] the removal of the templates may cause damage to the micro/nanocrystals as mentioned above. The present method opens up a facile route to the ultralong and pure micro/nanocrystals of molecular conductors. The size of the micro/nanocrystals can be tuned either by controlling the temperature or time for electrocrystallization.

---

(11) Valade, L.; de Caro, D.; Savy, J.-P.; Malfant, I.; Faulmann, C.; Almeida, M.; Fraxedas, J.; Brooks, J. *J. Low Temp. Phys.* **2006**, *142*, 393–396.

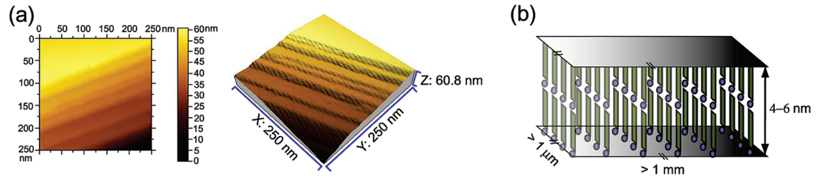

Figure 2. (a) AFM images of micro/nanocrystals of $\mathbf{4}_2\cdot FeCl_4$, where *X*, *Y*, and *Z* correspond to the length, width, and thickness of micro/nanocrystals, respectively; and (b) schematic depiction of the molecular arrays in micro/nanocrystals. The green rectangles and blue circles indicate the donor molecules **4** and counter $FeCl_4^-$ ions, respectively.

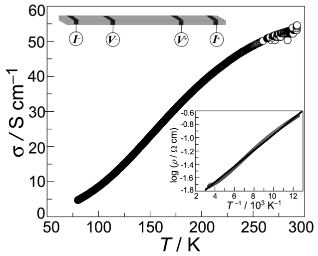

Figure 3. Temperature-dependent conductivity of $\mathbf{4}_2\cdot FeCl_4$ measured on the microcrystal. The bottom insert depicts the Arrhenius plot.

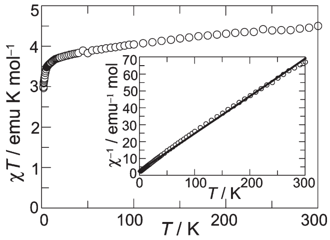

Figure 4. Temperature dependence of the χT product of $\mathbf{4}_2\bullet FeCl_4$ (χ, magnetic susceptibility). The insert depicts the thermal variation of χ^{-1} (open circle), and the Curie–Weiss fit (solid line).

The temperature-dependent resistivity of micro/nanocrystals of $\mathbf{4}_2\cdot FeCl_4$ was measured by conventional four-probe method along the crystal long axis on several pieces of microcrystals ($\sim 800 \times 3 \times 0.1\ \mu m^3$). The gold wires with diameter of 10 μm were attached to the crystal surface using carbon paste (see the top insert of Figure 3 for the schematic depiction). All of the micro/nanocrystals exhibited semiconducting behavior as shown in Figure 3. However, the room temperature conductivity is considerably high, around 40−60 S cm^{-1}. The activation energy for electric conduction is about 10 meV. Along with their good flexibility, the highly conducting property implies that the present micro/nanocrystals are good candidates as molecular wires. Note that the bulk platelet crystal also exhibited a semiconducting behavior with the room-temperature conductivity of 30 S cm^{-1} and activation energy of about 20 meV. The slight difference of the electronic transport properties between the micro/nanocrystals and bulk crystals is most plausibly due to the quality of the crystals, where the former should have fewer defects than the latter. Although all of the radical cation salts so far obtained based on **1**,[4c,9] **3**,[10] and **4** exhibit semicoducting behavior, the room temperature conductivities of the salts for these three donor molecules increase in the order of **1** (ca. 2 S cm^{-1}) < **3** (ca. 5 S cm^{-1}) < **4** (ca. 50 S cm^{-1}). This tendency may be due to the introduction of the large-sized chalcogen atoms which enhance the intracolumnar intermolecular interactions. In fact, the calculated intracolumnar interactions in the radical cation salts of **3** are larger than those in the salts of **1**.[4c,9,10]

The temperature-dependent magnetic susceptibility (χ) for the micro/nanocrystals of $\mathbf{4}_2\cdot FeCl_4$ was measured on a SQUID magnetometer applying the field of 1000 Oe. The temperature dependence of χ followed the Curie−Weiss law, $\chi = C/(T - \theta)$, with $C = 4.46$ emu K mol^{-1} and $\theta = -8.5$ K, which indicates that the d-spins of $FeCl_4^-$ ions show relatively strong antiferromagnetic interaction (Figure 4). This behavior is very similar to those of the magnetic conductors based on donor molecules **1** and **3**.[4c,9,10] The antiferromagnetic interaction of d-spins is most plausibly due to the preferential d−π−π−d interaction between the donor molecules **4** and counter $FeCl_4^-$ ions as proved in the $\mathbf{1}_2\cdot FeCl_4$ salt.[4c]

It is worth noting that by using the similar concept, the microcrystals of $\mathbf{2}_2\cdot FeCl_4\cdot(DCE)_{0.5}$ were also obtained by electrocrystallization without any templates (see Figure S2 in the Supporting Information). In this case, donor molecule **2** (2.0 mg) was electrochemically oxidized in the presence of $Bu_4N\cdot FeCl_4$ (35 mg) in 1,2-dichloroethane (DCE) applying the constant current of 1.0 μA at −5 °C under argon atmosphere. Further investigation on the preparation of ultralong microcrystals of $\mathbf{2}_2\cdot FeCl_4\cdot(DCE)_{0.5}$ and their transport properties is in progress.

In summary, the bent donor molecules **1**, **2**, **3**, and **4** have a strong tendency to form the 1D columns along the molecular face-to-face array. By fine-tuning of the experimental conditions, we could obtain the micro/nanocrystals of the magnetic molecular conductors based on **2** and **4** by electrocrystallization on the Pt rod without any templates. This novel approach may also be used to the other donor molecules which show the strong tendency to stack along a specific direction. The good flexibility and high conductivity of $\mathbf{4}_2\cdot FeCl_4$ make it an excellent candidate as molecular wires.

Acknowledgment. The authors are grateful to Dr. H. Yashiro (Rigaku Co., Japan) for the measruement of the powder XRD. This work is supported by a Grant-in-Aid for Scientific Research (No. 19350073) from the Ministry of Education, Culture, Sports, Science and Technology of Japan. The Collaboration between the Japanese and French groups is supported by the CNRS-GDRI 91 program on Multifunctional Molecular Materials and Devices.

Supporting Information Available: SEM-EDX results for micro/nanocrystals of $\mathbf{4}_2\cdot FeCl_4$ and $\mathbf{2}_2\cdot FeCl_4\cdot(DCE)_{0.5}$, and XRD patterns of $\mathbf{4}_2\cdot FeCl_4$ (PDF). This material is available free of charge via the Internet at http://pubs.acs.org.